

Schottky diodes using as-grown single-walled carbon nanotube ensembles

D. M. N. M. Dissanayake and Zhaohui Zhong

Citation: *Applied Physics Letters* **104**, 123501 (2014); doi: 10.1063/1.4869551

View online: <http://dx.doi.org/10.1063/1.4869551>

View Table of Contents: <http://scitation.aip.org/content/aip/journal/apl/104/12?ver=pdfcov>

Published by the [AIP Publishing](#)

The advertisement features a dark blue background with a central image of the Model PS-100 probe station. On the left, the text 'NEW Model PS-100 Preconfigured Tabletop Probe Station' is written in white and orange. On the right, the Lake Shore CRYOTRONICS logo is shown, followed by the tagline 'An affordable solution for a wide range of research' in a white, italicized font.

NEW
Model PS-100
Preconfigured Tabletop
Probe Station

 **Lake Shore**
CRYOTRONICS

*An affordable solution for
a wide range of research*

Schottky diodes using as-grown single-walled carbon nanotube ensembles

D. M. N. M. Dissanayake^{1,a)} and Zhaohui Zhong²

¹*Sustainable Energy Technologies Department, Brookhaven National Laboratory, Upton, New York 11973, USA*

²*Department of Electrical Engineering and Computer Science, University of Michigan, Ann Arbor, Michigan 48109, USA*

(Received 3 February 2014; accepted 7 March 2014; published online 25 March 2014)

We demonstrate rectifying Schottky diodes fabricated using as-grown single-walled carbon nanotubes (SWNT) ensembles, without removing the metallic SWNTs, for optoelectronic device applications. The SWNTs are contact by a low work-function metal through a high-bandgap charge-blocking layer (ZnO) resulting in highly-nonlinear current-voltage properties compared to control ensemble SWNT devices, fabricated without a charge-blocking layer, which show resistive behaviour. This significant improvement in diode behaviour is obtained by reducing source-drain leakage from the metallic SWNTs using the charge-blocking layer which channels charge transport via the semiconducting SWNTs. Moreover, we explore an alternative method of creating the charge barrier layer via oxidizing a thin film of Zn deposited on directly on the SWNTs which could potentially reduce cost and increasing scalability of this technique to obtain highly rectifying diodes from as-grown ensemble SWNTs. © 2014 AIP Publishing LLC. [<http://dx.doi.org/10.1063/1.4869551>]

Single-walled carbon nanotubes (SWNTs) have strong light absorption property, spanning a broad spectrum from the ultraviolet to the near-infrared wavelengths, through direct inter-subband optical transitions.^{1,2} In addition, SWNTs have weak elastic scattering and suppressed inelastic scattering at low bias resulting in a mean-free path and a carrier mobility of $\sim 0.5 \mu\text{m}$ and $10^5 \text{ cm}^2 \text{ V}^{-1} \text{ s}^{-1}$, respectively.^{3,4} Apart from these unique optical and electrical properties, SWNT also demonstrates superior mechanical and chemical stability ideal for high performance, low-cost, and lightweight optoelectronics devices.^{5,6} In particular, there is a significant interest in using SWNTs as the active material for novel photovoltaic applications.^{7,8} A unique property of SWNTs in converting single absorbed photons to multiple electron-hole pairs could make SWNT photovoltaics operate with power conversion efficiencies exceeding the Shockley-Queisser upper limit.⁹

In order to generate photocurrent, excitons created in a SWNT—with a binding energy of 300–400 meV⁹—have to dissociate into free charge carriers.¹⁰ In a SWNT based photovoltaic, exciton dissociation occurs at the semiconducting (s-) SWNT and (m-) metal Schottky junction^{10–12} when the built-in field at the junction is greater than the exciton binding energy.¹¹ Driven by the simpler design and well understood physics of bulk semiconductor-metal interfaces, Schottky based SWNT photovoltaics might be possible candidates for large area photovoltaic devices. However, Schottky junctions with sufficient built-in potential to dissociate excitons (i.e., $>400 \text{ meV}$) cannot be created between small-bandgap SWNT (sb-SWNT) (i.e., band-gap less than 400 meV) or metallic (m-) SWNT based SWNT and metal interfaces. Since as-grown ensemble of SWNTs is approximately 30% metallic SWNTs,¹³ fabrication of non-linear devices using as-grown ensembles of SWNTs with significant rectification and a built-in potential for photocurrent generation is challenging. One solution is to

remove the m-SWNT via post-synthesis purification methods, thereby isolating a high percentage of pure s-SWNT for fabricating near ideal Schottky junctions.¹⁴ Alternating-current dielectrophoresis,¹⁵ buoyancy in structure-discriminating surfactants,¹⁶ as well as organic polymers with specific bindings to selectively dissolve s-SWNT¹⁷ are examples of the techniques explored in lowering m-SWNTs from as-grown SWNT ensembles. However, such filtering techniques are not applicable for on-wafer grown SWNT films (typically synthesised via a chemical vapour deposition method) suitable for integrated SWNT based device fabrication. For these devices, removal of m-SWNT has been attempted by selectively burning m-SWNT under applied high bias,¹¹

In this paper, we demonstrate highly rectifying as-grown ensemble SWNT-metal junctions without physically removing the m-SWNTs from the as-grown SWNT ensemble. We use an undoped ZnO barrier layer that restricts charge transport through the m-SWNTs, without affecting transport via the s-SWNTs, to demonstrate significantly improved the non-linear electrical performance in ensemble SWNTs-metal Schottky diodes. As the m-SWNTs become electrically isolated, the Schottky built-in potential is determined by the larger-bandgap s-SWNT/metal junction, making exciton dissociation and photocurrent generation possible in the ensemble-SWNT diodes. Furthermore, we demonstrate an alternative deposition method of the ZnO barrier layer using a low-cost and highly scalable process of oxidizing thin-film of metallic Zn deposited directly on the as-grown SWNTs.

The schematic band diagram shown in Fig. 1(a) explains the principle of operation of the proposed ensemble-SWNT Schottky diode with Pd (drain) and Al (source) electrodes together with a ZnO charge barrier layer. The valence energy level of the s-SWNT form an ohmic contact with the Pd electrode, and at the other end a Schottky junction is formed with the low work-function Al.¹¹ The Schottky junction can still form even in the presence of an ultrathin hole blocking layer (i.e., ZnO) between the s-SWNT and Al. In this device

^{a)}Author to whom correspondence should be addressed. Electronic mail: ndissanayake@bnl.gov

architecture, the photogenerated electrons can be extracted under the built-in field at the Al contact via the conduction band of ZnO. However, charge transport via the sb-SWNT or m-SWNT is completely blocked by the wide-bandgap blocking layer (ZnO). Conduction via the m-SWNT at Fermi Energy (4.7 eV (Ref. 18)) is blocked due to the nearly zero density of states within the mid-gap of the ZnO, and the sb-SWNTs form a large potential barrier with the conduction band of the ZnO (4.5 eV) mitigating electron transport. As a result, both m-SWNT and sb-SWNT become isolated from charge transport within this ensemble of SWNTs making s-SWNTs solely responsible for the overall electrical behaviour in the diode.

A schematic of the fabricated device structure is shown in Fig. 1(b). The SWNTs with an average diameter of ~ 1.5 nm, shown by atomic force micrograph in Fig. 1(c), were synthesised using chemical vapour deposition on quartz substrates patterned with 0.3 nm Fe catalysts.¹⁹ Growth of SWNT was carried out at 900° in a 1 in. tube furnace using

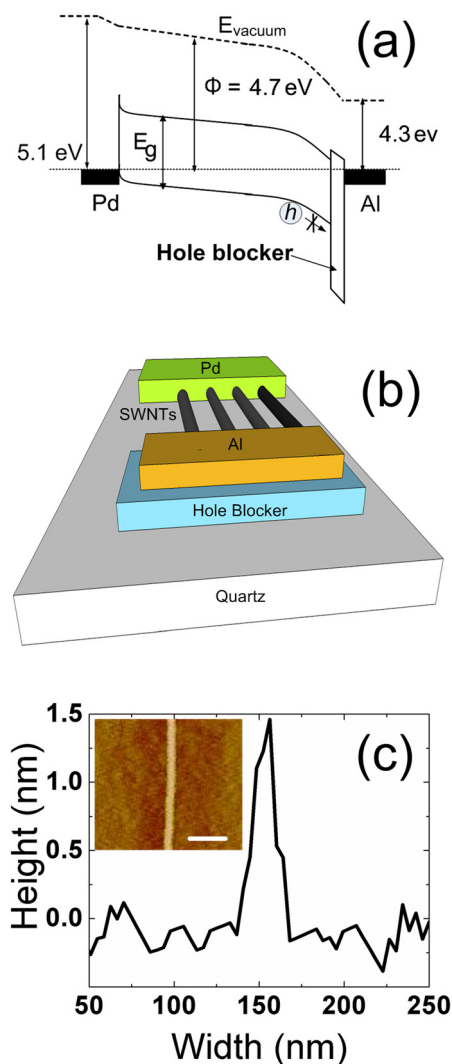


FIG. 1. SWNT Schottky devices fabricated with a hole blocking ZnO layer. (a) Flat band diagram of Pd/ensemble-SWNTs/ZnO/Al device. (b) Schematic of the Schottky diode SWNT device fabricated on a quartz substrate. ZnO layer is either deposited using pulse laser deposition method or oxidizing a metallic thin film of Zn layer deposited using e-beam evaporation. (c) Atomic Force Micrograph of the showing the height (~ 1.5 nm) of an individual SWNT found in the ensemble. (Scale bar 100 nm)

CH₄ (1900 sccm) and H₂ (300 sccm) at ambient pressure for 60 min. Samples were characterized using atomic force microscopy (AFM) (Veeco Dimension 3100). SWNT density, obtained by this recipe was approximately 1-SWNT per 15- μm^2 of catalyst area. Therefore, we are able to control the number of SWNT per device by choosing an appropriate catalyst area; i.e., to fabricate ensemble vs. individual SWNT diodes we use 150- μm^2 vs. 15- μm^2 area, respectively. SWNT Schottky junction two-terminal devices were fabricated by evaporating Pd and Al contacts patterned by photolithography, forming ensemble SWNT channel length of ~ 3 μm . Prior to depositing the Al contact, a thin layer of undoped ZnO is deposited using pulse laser deposition as explained in the previous work.²⁰

Fig. 2(a) shows AFM of the channel area of an ensemble SWNTs (~ 10) diode with Pd and ZnO/Al drain and source electrodes on a quartz substrate. A 20 nm undoped ZnO layer was deposited using pulse laser deposition. Fig. 2(b) shows the current-voltage (I-V) characteristics of 5 diodes each on average having ~ 10 SWNTs. Each as-grown ensemble SWNT device shows non-linear diode behaviour. In comparison, the control ensemble-SWNT Schottky diode, prepared identically (Fig. 2(b) inset) without the ZnO layer, shows the expected completely linear I-V behaviour with ~ 7.5 k Ω resistance. Therefore, as predicted the ZnO barrier blocks the transport via the m-SWNT and sb-SWNT producing highly nonlinear diode IV characteristics.

We further investigate an alternative method of depositing intrinsic ZnO which is low cost, scalable, and which can be used readily with the nano-fabrication methods. We oxidized a thin-film of Zn which is directly deposited on the SWNTs, under ambient conditions to obtain a thermally oxidized ZnO, denoted ZnO_t, hole blocking layer. On top of substrates having SWNTs as described above, 5 nm thick Zn was deposited on patterned areas defined by photolithography. Afterwards, the substrates were thermally annealed in

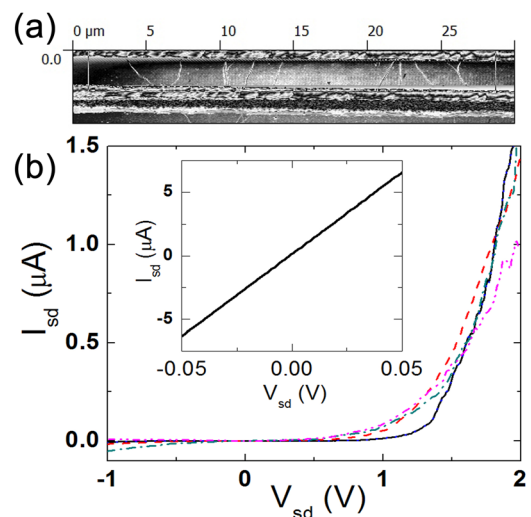


FIG. 2. (a) AFM of as-grown ensembles of SWNTs (~ 10) crossing a Pd and ZnO/Al contact. (b) I-V characteristics of Pd/SWNTs/ZnO/Al devices consisting of multiple SWNT crossing the source-drain channel fabricated with the charge blocking ZnO layer synthesised using pulse laser deposition. (Inset) I-V characteristics of the Pd/SWNT/Al control device fabricated with Pd and Al drain and source contact, without the ZnO layer.

air at 300° for 5 min. Conversion of Zn to ZnO_t was qualitatively determined by observing a distinct change in colour from the dull-grey (indicating Zn) to near transparent (indicating a higher bandgap ZnO) using an optical microscope. Afterwards, the source (Al) and drain (Pd) contacts were deposited following as described earlier.

Fig. 3(a) shows the IV characteristics the Pd/SWNTs/ZnO_t (5 nm)/Al device which is having similar SWNT count (~10) to Fig 2. As synthesised, the device shows a linear I-V (solid-line) which indicates that the ZnO_t layer is highly conductive. However, after annealing the whole device for (350°C for 1 min) under ambient conditions, the I-V characteristics transformed from a linear to non-linear diode behaviour (dashed-line). Using the low bias region of the I-V curve and fitting to an ideal-diode equation $I = I_s(\exp(qV/\eta kT) - 1)$, where I_s is the reverse saturation current, q is the charge of an electron, V is the bias voltage, k is the Boltzmann constant, and T is the absolute temperature, the η (ideality factor) is obtained as 3.0 (inset). We postulate that, post-deposition annealing must have further passivated the trap-states and/or stoichiometry inhomogeneity of the ZnO_t thereby improving the dielectric behaviour of the hole-blocking layer. As a result, a dramatic enhancement of

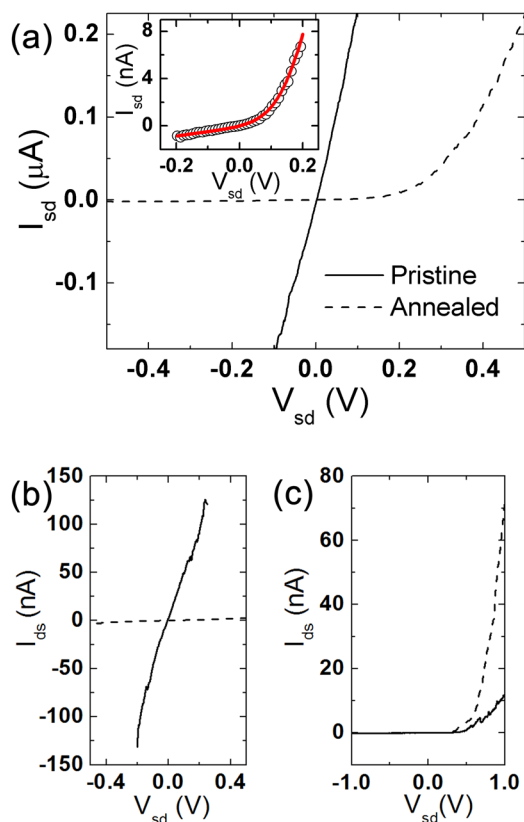


FIG. 3. I-V characteristics of the Pd/SWNTs/ZnO(5 nm)/Al diodes where metallic Zn converted to ZnO via thermal annealing. Black solid line (dashed) line represents current-voltage behaviour obtained before (after) post-fabrication thermal annealing at 350°C for 1 min, respectively. (a) I-V characteristics of a Pd/SWNTs/ZnO(5 nm)/Al device having an ensemble of SWNTs (~10) in the channel. Inset shows a theoretical fitting to the low bias region to obtain the ideality factor of the diode after annealing. (b) and (c) show the I-V characteristics of a Pd/SWNT/ZnO(5 nm)/Al diodes consisting a single SWNT with linear (corresponding to a metallic or small-bandgap SWNT) and non-linear (corresponding to a larger bandgap semiconducting SWNT), respectively.

the non-linear behaviour of the Pd/SWNTs/ZnO_c (5 nm)/Al is obtained.

Furthermore, we looked into the effect of a hole blocking layer (ZnO_t) on diodes having only a single SWNT between Pd and ZnO_t/Al contacts. Channels with single SWNT were selected from characterizing the 15 μm^2 catalyst areas after growth using AFM and Scanning Electron Microscopy. Fig. 3(b) shows a single SWNT device which showed linear I-V, with a conductance of 0.5 μS , prior to post-deposition thermal annealing (solid-line) indicating that the SWNT is either a small bandgap or metallic in nature. Upon post-deposition annealing at 350° for 1 min, the conductance of the device is reduced by two orders of magnitude to 5.4 nS. Therefore, the impact of the ZnO_t to the transport of the sb-SWNT or m-SWNT is clearly evident from the above. The small residual conductance can be attributed to leakage pathways through the barrier due to non-uniformity in the film and also the presence of defects.

We also looked in to the comparative behaviour of the ZnO_t barrier layer on the transport of an individual SWNT with non-linear I-V characteristics prior to annealing, which is expected behaviour from s-SWNT as shown in Fig 3(c). Prior to post-deposition annealing, the ideality factor of the diode is 3.7. Upon post-deposition annealing, η reduces to 3.0 suggesting that the hole-barrier layer has further mitigated minority carrier recombination at the junction. Furthermore, the forward bias conductance of the diode is also increased from 20 nS to 166 nS which can be attributed to the improvement of the ohmic behaviour at the drain (Pd) contact. As a result, using the individual SWNT diodes, we are able to confirm the effect of the ZnO barrier layer on the charge transport of the various SWNT species, explaining the observed ensemble SWNT diode I-Vs shown in Figs. 2 and 3(a).

In conclusion, in this paper we investigated the effect of a hole-barrier (ZnO) on the charge transport of an as-grown ensemble-SWNT diode, which converts the device properties from linear to highly non-linear diode characteristics useful for SWNT applications. Furthermore, we proposed an alternative method of thermally oxidizing such a barrier layer, which could prove a lower-cost and simpler technique for device fabrication. We believe that use of this type of a charge barrier can facilitate the fabrication of the ensemble-SWNT which can be used for various optoelectronic devices in the future.

We like to acknowledge Professor John Hart and Professor Jamie Phillips help in the device fabrication and pulse-laser deposition of ZnO. We thank the support from the UoM/SJTU Collaborative Research Program in Renewable Energy Science and Technology. This work used the Lurie Nanofabrication Facility at the University of Michigan, a member of the National Nanotechnology Infrastructure Network funded by the National Science Foundation.

¹T. Odom, J. Huang, P. Kim, and C. Lieber, *Nature* **391**, 62 (1998).

²J. Wildoer, L. Venema, A. Rinzler, R. Smalley, and C. Dekker, *Nature* **391**, 59 (1998).

- ³R. Saito, G. Dresselhaus, and S. Dresselhaus, *Physical Properties of Carbon Nanotubes* (Imperial College Press, 1998).
- ⁴M. Freitag, V. Perebeinos, J. Chen, A. Stein, J. C. Tsang, J. A. Misewich, R. Martel, and P. Avouris, *Nano Lett.* **4**, 1063 (2004).
- ⁵P. Avouris, Z. Chen, and V. Perebeinos, *Nat. Nanotechnol.* **2**, 605 (2007).
- ⁶P. Avouris, M. Freitag, and V. Perebeinos, *Nat. Photonics* **2**, 341 (2008).
- ⁷R. M. Jain, R. Howden, K. Tvrđy, S. Shimizu, A. Hilmer, T. P. McNicholas, K. K. Gleason, and M. S. Strano, *Adv. Mater.* **24**, 4436 (2012).
- ⁸M. S. Arnold, J. L. Blackburn, J. J. Crochet, S. K. Doorn, J. G. Duque, A. Mohite, and H. Telg, *Phys. Chem. Chem. Phys.* **15**, 14896 (2013).
- ⁹J. Maultzsch, H. Telg, S. Reich, and C. Thomsen, *Phys. Rev. B* **72**, 205438 (2005).
- ¹⁰M. Freitag, Y. Martin, J. A. Misewich, R. Martel, and P. Avouris, *Nano Lett.* **3**, 1067 (2003).
- ¹¹C. Chen, Y. Lu, E. S. Kong, Y. Zhang, and S.-T. Lee, *Small* **4**, 1313 (2008).
- ¹²Y. Ma, L. Valkunas, S. Bachilo, and G. Fleming, *J. Phys. Chem. B* **109**, 15671 (2005).
- ¹³M. Zheng, A. Jagota, M. S. Strano, A. P. Santos, P. Barone, S. G. Chou, B. A. Diner, M. A. Dresselhaus, R. S. Mclean, G. B. Onoa *et al.*, *Science* **302**, 1545 (2003).
- ¹⁴F. Lu, M. J. Meziani, L. Cao, and Y.-P. Sun, *Langmuir* **27**, 4339 (2011).
- ¹⁵R. Krupke, F. Hennrich, H. von Lohneysen, and M. Kappes, *Science* **301**, 344 (2003).
- ¹⁶M. S. Arnold, A. A. Green, J. F. Hulvat, S. I. Stupp, and M. C. Hersam, *Nat. Nanotechnol.* **1**, 60 (2006).
- ¹⁷H. W. Lee, Y. Yoon, S. Park, J. H. Oh, S. Hong, L. S. Liyanage, H. Wang, S. Morishita, N. Patil, Y. J. Park *et al.*, *Nat. Commun.* **2**, 541 (2011).
- ¹⁸K.-i. Okazaki, Y. Nakato, and K. Murakoshi, *Phys. Rev. B* **68**, 035434 (2003).
- ¹⁹J. Kong, H. Soh, A. Cassell, C. Quate, and H. Dai, *Nature* **395**, 878 (1998).
- ²⁰W. E. Bowen, W. Wang, and J. D. Phillips, *IEEE Electron. Dev. Lett.* **30**, 1314 (2009).